

The following article appeared in Energy Reports, 6: 1170-1180 (2020) and may be found at: <https://doi.org/10.1016/j.egy.2020.04.038>

This is an open access article under the Creative Commons Attribution-NonCommercial-NoDerivatives 4.0 International (CC BY-NC-ND 4.0) license. <https://creativecommons.org/licenses/by-nc-nd/4.0/>



Research paper

Biohydrogen production from cheese whey powder by *Enterobacter asburiae*: Effect of operating conditions on hydrogen yield and chemometric study of the fermentative metabolites



Cecilia L. Alvarez-Guzmán^{a,1}, Sergio Cisneros-de la Cueva^{a,1},
 Víctor E. Balderas-Hernández^a, Adam Smoliński^b, Antonio De León-Rodríguez^{a,*}

^a División de Biología Molecular, Instituto Potosino de Investigación Científica y Tecnológica A.C., Camino a la Presa San José 2055, Lomas 4a Sección, Postal Code, 78216 San Luis Potosí, S.L.P., Mexico

^b Central Mining Institute, Pl. Gwarków 1, 40-166 Katowice, Poland

ARTICLE INFO

Article history:

Received 23 March 2020

Received in revised form 23 April 2020

Accepted 29 April 2020

Available online xxxx

Keywords:

Hydrogen

Dark fermentation

Agro-industrial wastes

RSM

Chemometrics

ABSTRACT

In this study, the response surface methodology (RSM) with a central composite design (CCD) was applied to evaluate the effect of temperature, initial pH and cheese whey powder concentration (CWP) on the hydrogen yield and hydrogen production rate by the *Enterobacter asburiae*. Batch fermentations were performed in 120 cm³ serological bottles with a working volume of 110 cm³. The CWP concentration evaluated was in a range of 4.8–55.2 g dm⁻³, initial pH in a range of 3.4–10.1 and temperatures of 4.8–55.2 °C. The maximum hydrogen yield and production rate of 1.19 ± 0.01 mol H₂ mol⁻¹ lactose and 9.34 ± 0.22 cm³ dm⁻³ h⁻¹, respectively were achieved at the optimum conditions of 25.6 °C, initial pH of 7.2 and 23.0 g dm⁻³ CWP. Moreover, a chemometric analysis was applied for the comparison and visualization of the effect of the different operating conditions on the distribution of the metabolites produced. According to the hierarchical clustering analysis (HCA), the production of acetic acid, formic acid and ethanol was stimulated mainly by low temperature conditions of 15 °C, while the production of reduced compounds such as succinic acid, lactic acid and 2,3-butanediol was favored by 30 °C, initial pH 6.8 and CWP concentrations ≥ 30 g dm⁻³.

© 2020 The Authors. Published by Elsevier Ltd. This is an open access article under the CC BY-NC-ND license (<http://creativecommons.org/licenses/by-nc-nd/4.0/>).

1. Introduction

The growing energy demand has caused serious environmental problems; this has created the necessity for replacing fossil fuels with sustainable energy sources (da Silva Veras et al., 2017; Lee, 2017). Hydrogen is now considered as one of the alternatives to fossil fuels. It is preferred over biogas or methane because it is not chemically bound to carbon, therefore the only product of its combustion is water (Azbar et al., 2009; Ferchichi et al., 2005). Also, it has a high-energy yield of 122 kJ g⁻¹, which is almost three times higher than hydrocarbon fuels (Rosales-Colunga et al., 2010). Although hydrogen has showed potential to be used for clean energy purposes, it is produced mostly by fossil fuel processing technologies; which are expensive and highly polluting due to the operating conditions (Holladay et al., 2009). Whereas in biological methods, hydrogen is produced by the metabolic transformation of a carbon source by a variety

of microorganisms under anaerobic dark fermentation (Mohan et al., 2013). This process has the advantage of not requiring direct solar input, of accepting a variety of inexpensive substrates, and using a very simple reactor technology (Bao et al., 2012). The application of cheap substrates on hydrogen production has been widely studied. Among a wide variety of economic carbon sources, cheese whey (CW), is a promising carbohydrate-rich substrate due to its nutritional characteristics which are beneficial for the hydrogen-producing bacteria (Prazeres et al., 2012). This waste is the by-product obtained from cheese production which represents around 85%–90% of the total volume of processed milk. It is estimated that 190 x 10⁶ tons year⁻¹ of CW are produced worldwide (Ryan and Walsh, 2016). Typical CW mainly contains lactose (4.5–5.0% w v⁻¹), soluble proteins (0.6–1.0% w v⁻¹), lipids (0.4–0.5% w v⁻¹), and mineral salts (6%–10% of dried extract) (Zhou et al., 2019). The low lactose content of CW requires processing large quantities of waste for H₂ gas production which represents an economic disadvantage (Kargi et al., 2012). On the contrary, cheese whey powder (CWP) is a concentrated and commercial form of CW. The use of CWP eliminates expensive ultrafiltration steps and has other considerable advantages over CW such as reduced volume, concentrated lactose content, long term

* Corresponding author.

E-mail addresses: aleonr@ipicyt.edu.mx, aleonr@me.com

(A. De León-Rodríguez).

¹ These authors contributed equally.

Table 1

Experimental range and levels of independent variables evaluated during hydrogen yield optimization.

| Variable | Units | − α | −1 | 0 | +1 | + α |
|----------|--------------------|------------|-----|-----|-----|------------|
| T | °C | 4.8 | 15 | 30 | 45 | 55.2 |
| pH | – | 3.4 | 4.8 | 6.8 | 8.8 | 10.1 |
| CW | g dm ^{−3} | 4.8 | 15 | 30 | 45 | 55.2 |

stability and easy storage and transportation (Kargi and Ozmihi, 2006). Several authors have reported the use of this substrate for hydrogen production by strict anaerobes such as *Clostridium saccharoperbutylacetonicum* (2.70 mol mol^{−1} lactose) (Ferchichi et al., 2005), mixed cultures (1.8 mol mol^{−1} lactose) (Vasmara and Marchetti, 2017) or facultative anaerobes such as *Escherichia coli* (1.78 mol mol^{−1} lactose) (Manuel Rosales-Colunga et al., 2013), or *E. aerogenes* (2.04 mol mol^{−1} lactose) (Rai et al., 2012). Among the fermentative hydrogen producers; bacteria belonging to *Enterobacter* genus are attractive due to their high hydrogen evolution rate and because they have two routes to produce hydrogen known as the formate pathway and NADH pathway (Lu et al., 2009). Even when *Enterobacter* is a genus widely studied for hydrogen production, to our knowledge, there is only one report addressing the use of a pure culture of *Enterobacter* with CW as substrate (Rai et al., 2012). Therefore, the aim of the present study was to evaluate the combined effects of temperature, initial pH and CWP concentration on the hydrogen production by *E. asburiae* applying the response surface methodology (RSM). In addition, a chemometric analysis of the experimental data concerning to the metabolites produced was applied with the aim to find and group various fermentation conditions which led to the different distribution of the metabolic products in each experimental set.

2. Materials and methods

2.1. Strain and culture media

E. asburiae was cultured at 25 °C in agar plates with growth medium containing in g dm^{−3} 0.25 yeast extract (Difco), 2.75 Bacto-tryptone (Difco), and 20 lactose (Sigma). For batch fermentation experiments, CWP used was purchased from Land O' Lakes Inc. (Minnesota, USA) with a composition as follows: 75% (w w^{−1}) lactose, 14.5% (w w^{−1}) protein, 1.5% (w w^{−1}) lipids and 8.8% (w w^{−1}) mineral salts. Before its use CWP was pasteurized during 30 min at 65 °C and chilled 20 min on ice.

2.2. Experimental design

A central composite design (CCD) 2³ was applied to determine the effect of temperature (°C), initial pH and initial CWP concentration (g dm^{−3}) on the hydrogen yield and production rate by *E. asburiae*. The levels of the evaluated factors are listed in Table 1 and the design matrix with the corresponding hydrogen yield and production rate results are presented in Table 2. The empirical second order polynomial model was applied (Eq. (1)) to build surfaces graphs and to predict the optimum conditions:

$$Y = \beta_0 + \sum_{i=1}^k \beta_i X_i + \sum_{i=1}^k \beta_{ii} X_i^2 + \sum_{i=1}^{k-1} \sum_{j=2}^k \beta_{ij} X_i X_j \quad (1)$$

where Y is the predicted response, β_0 is the model intercept, β_i is the linear coefficient, β_{ii} is the interaction coefficient, β_{ij} is the interaction coefficient, whereas X_i X_j are independent variables (Gunst et al., 1996). The experimental design and the statistical analysis were performed with the Design Expert v7.0 software.

2.3. Batch fermentations

Pre-inocula of *E. asburiae* were grown in liquid medium containing in g dm^{−3} 20 lactose, 0.25 yeast extract (Difco) and 2.75 g dm^{−3} Bacto-tryptone. Cells were harvested, washed and inoculated into 120 cm³ serological bottles (Prisma, DF, Mex) containing 110 cm³ of production medium with the corresponding CWP concentration according to Table 2. Production medium consisted in g dm^{−3} of: 0.25 yeast extract (Difco) and 2.75 Bacto-Tryptone (Difco) supplemented with 1 cm³ dm^{−3} of trace elements solution with a composition in g dm^{−3}: 0.015 FeCl₃·4H₂O, 0.00036 Na₂MoO₄·2H₂O, 0.00024 NiCl₂·H₂O, 0.0007 CoCl₂·6H₂O, 0.0002 CuCl₂·2H₂O, 0.0002 Na₂SeO₃ and 0.01 MgSO₄. Cultures were started at an initial optical density at 600 nm wavelength (O.D._{600nm}) of 0.5. Initial pH was adjusted in each serological bottle according to the experimental design (Table 2). Silicon stoppers and screw caps were used to avoid gas leakage from the bottles.

2.4. Analytical methods

The volume of biogas produced was measured periodically by the acidic water (pH < 2) displacement method in an inverted burette connected to the serological bottles using a rubber tubing and a needle. The percentage of hydrogen in the gas was measured using a gas chromatograph (6890N, Agilent Technologies), equipped with a thermal conductivity detector and using an Agilent J&W HP-Plot Molesieve column (30 m x 0.32 mm i.d. x 12 μm film thickness). Liquid samples of 1 cm³ were taken, diluted and filtered using a 0.22 μm syringe filter. The final concentration of lactose, formic acid, and acetic acid were determined using a High-Performance Liquid Chromatograph (HPLC, Infinity LC 1220, Agilent Technologies) with a refraction index detector (Agilent Technologies) and a column Rezex ROA (Phenomenex, Torrance) at 60 °C, and 0.0025 M H₂SO₄ as mobile phase at 0.05 cm³ min^{−1}. The final concentrations of ethanol and 2,3-butanediol were determined using a gas chromatograph (GC, 6890N, Agilent Technologies) with a flame ionization detector (Agilent Technologies). The capillary column HP-Innowax (30 m x 0.25 μm i.d. x 0.5 μm film thickness, Agilent Technologies) was used to perform the analysis.

2.5. Data organization and methods of data exploration

The studied experimental data set was organized into matrix \mathbf{X} (16 x 6), which rows represent 16 objects (experiments of hydrogen production under various conditions), whereas the columns correspond to the studied parameters (metabolites produced in CWP fermentation), listed in Table 3. The studied data was centered and standardized before principal component analysis (PCA) (Djaković Sekulić et al., 2016; Howaniec et al., 2015; Jolliffe, 2002; Smoliński, 2011; Wold et al., 1987), and hierarchical clustering analysis (HCA) (Gentle et al., 1991; Howaniec et al., 2015; Milligan and Romesburg, 1985; Smoliński, 2008) models were constructed. The PCA and HCA are the methods most often applied in data exploration. PCA allows reducing data dimensionality and visualization of the studied data by projection of objects and parameters on the space defined by the score and loading vectors (Djaković Sekulić et al., 2016; Howaniec et al., 2015; Jolliffe, 2002; Smoliński, 2011; Wold et al., 1987). It enables to decompose the data of a matrix \mathbf{X} (m x n) into two matrices, \mathbf{S} (m x fn) and \mathbf{D} (n x fn), called score and loading matrices, respectively, where m and n denote the number of objects and parameters, respectively, whereas fn denotes the number of significant factors called the Principal Components (PCs). The hierarchical clustering analysis (Gentle et al., 1991; Howaniec et al., 2015; Milligan

Table 2
Experimental conditions of the CCD and the corresponding hydrogen yield and production rate results.

| Exp. | Temperature (°C) | pH (–) | CWP (g dm ⁻³) | Lactose content (g dm ⁻³) | H ₂ yield (mol H ₂ mol ⁻¹ lactose) | H ₂ yield (mol H ₂ mol ⁻¹ lactose) predicted | H ₂ production rate (cm ³ dm ⁻³ h ⁻¹) | H ₂ production rate (cm ³ dm ⁻³ h ⁻¹) predicted |
|------|------------------|--------|---------------------------|---------------------------------------|---|---|--|--|
| 1 | 30 | 6.8 | 4.8 | 3.6 | 0.76 | 0.97 | 5.65 | 6.24 |
| 2 | 15 | 4.8 | 15 | 11.3 | 0.056 | 0.07 | 0.33 | 0.28 |
| 3 | 45 | 4.8 | 15 | 11.3 | 0 | 0.00 | 0 | 0.08 |
| 4 | 15 | 8.8 | 15 | 11.3 | 0.71 | 0.23 | 2.91 | 1.32 |
| 5 | 45 | 8.8 | 15 | 11.3 | 0 | 0.00 | 0 | 0.02 |
| 6 | 30 | 3.4 | 30 | 22.5 | 0 | 0.00 | 0 | 0.00 |
| 7 | 4.8 | 6.8 | 30 | 22.5 | 0 | 0.02 | 0 | 0.17 |
| 8 | 30 | 6.8 | 30 | 22.5 | 1.22 | 1.22 | 10.23 | 10.43 |
| 9 | 30 | 6.8 | 30 | 22.5 | 1.23 | 1.22 | 10.59 | 10.43 |
| 10 | 55.2 | 6.8 | 30 | 22.5 | 0 | 0.00 | 0 | 0.00 |
| 11 | 30 | 10.1 | 30 | 22.5 | 0 | 0.02 | 0 | 0.11 |
| 12 | 15 | 4.8 | 45 | 33.8 | 0.01 | 0.01 | 0.12 | 0.09 |
| 13 | 45 | 4.8 | 45 | 33.8 | 0 | 0.02 | 0 | 0.12 |
| 14 | 15 | 8.8 | 45 | 33.8 | 0.07 | 0.05 | 1.80 | 1.02 |
| 15 | 45 | 8.8 | 45 | 33.8 | 0.05 | 0.04 | 0.10 | 0.14 |
| 16 | 30 | 6.8 | 55.2 | 41.4 | 0.80 | 0.68 | 6.96 | 6.20 |

Table 3
Matrix X (16 x 16) of the metabolites formed during the fermentations by *E. asburiae* under different experimental conditions.

| Objects | Parameters | | | | | |
|---------|-----------------------------------|-------------------------------------|-----------------------------------|-----------------------------------|---------------------------------------|-------------------------------|
| | Lactic acid (g dm ⁻³) | Succinic acid (g dm ⁻³) | Formic acid (g dm ⁻³) | Acetic acid (g dm ⁻³) | 2, 3-butanediol (g dm ⁻³) | Ethanol (g dm ⁻³) |
| 1 | 0.034 | 0.098 | 0.144 | 0.421 | 0.509 | 0.824 |
| 2 | 0.033 | 0.162 | 0.255 | 0.665 | 0.051 | 5.021 |
| 3 | 0.068 | 0.394 | 0.532 | 0.447 | 0.082 | 0.625 |
| 4 | 0.033 | 0.321 | 0.376 | 0.773 | 0.931 | 6.036 |
| 5 | 0.097 | 0.296 | 0.052 | 0.507 | 0.901 | 0.191 |
| 6 | 0.059 | 0.000 | 0.000 | 0.000 | 0.000 | 0.715 |
| 7 | 0.056 | 0.193 | 0.000 | 0.037 | 0.000 | 0.511 |
| 8 | 0.095 | 0.601 | 0.000 | 0.773 | 5.422 | 1.717 |
| 9 | 0.098 | 0.713 | 0.000 | 0.665 | 5.732 | 1.610 |
| 10 | 0.058 | 0.000 | 0.000 | 0.000 | 0.000 | 0.000 |
| 11 | 0.031 | 0.000 | 0.000 | 0.000 | 0.000 | 0.000 |
| 12 | 0.033 | 0.280 | 0.407 | 0.510 | 0.058 | 5.326 |
| 13 | 0.053 | 0.053 | 0.038 | 0.614 | 0.082 | 0.355 |
| 14 | 0.050 | 0.492 | 0.501 | 0.200 | 0.964 | 6.347 |
| 15 | 0.051 | 0.043 | 0.065 | 0.451 | 0.112 | 0.782 |
| 16 | 0.082 | 0.698 | 0.366 | 0.608 | 5.379 | 1.429 |

and Romesburg, 1985; Smoliński, 2008) allows investigating the similarities between studied objects in the parameter space, and between the parameters in the object space. The results of HCA are presented in the form of dendrograms differing in terms of the applied similarity measure between objects, as well as the way the similar objects are connected. The linkage methods include the single linkage, average linkage, complete linkage, centroid linkage and Wards linkage method (Gentle et al., 1991; Milligan and Romesburg, 1985). To complement the analysis of HCA and to determine the relationships between objects in the parameters space and parameters in the objects space, a color map of the experimental data enabling a more in-depth interpretation of the data structure, and parallel tracing the similarities between studied objects and parameters was employed (Smoliński, 2014, 2008).

3. Results and discussion

3.1. Hydrogen yield under different operating conditions

The RSM was applied with the aid of a CCD in order to obtain the optimum combined effect of temperature, initial pH and CWP concentration on hydrogen yield by *E. asburiae*. In Table 2, the different experimental conditions evaluated and the respective hydrogen yield results are shown. According to the analysis of the Box–Cox plot, a data transformation was required to ensure that the model meets the assumptions required for the analysis of variance (ANOVA). Therefore, a natural Log transformation was

applied. The ANOVA of the optimization study (Table 4) showed that hydrogen yield was significantly affected ($p < 0.05$) by the quadratic terms of temperature and pH. As showed in Table 2, the highest hydrogen yield (1.23 ± 0.01 mol H₂ mol⁻¹ lactose) was reached by the central points (Exp. 8 and 9) of the experimental design at 30 °C, pH 6.8 and 30 g dm⁻³ of CWP. Experiments 1 and 16 with the axial points of CWP concentration, 30 °C and initial pH 6.8, together with experiment 4, showed hydrogen yields in a range of 0.71–0.80 mol H₂ mol⁻¹ lactose. Moreover, lower yields in a range of 0.01–0.07 mol H₂ mol⁻¹ lactose were obtained by experiments 2, 12 and 14 at 15 °C along with experiment 15 at 45 °C. On the other hand, the pair of experiments 7 and 10 and 6 and 11 with the axial points of temperature and pH, respectively, showed no hydrogen production. The same was observed in experiments 3, 5 and 13 at 45 °C.

The final second-order-polynomial in terms of the coded factors after the natural Log transformation is expressed as follows:

$$\begin{aligned} \ln(Y_{H_2} + 0.01) = & 0.21 - 0.49T + 0.38pH - 0.11CWP \\ & - 0.24T * pH + 0.61T * CWP + 0.056pH * \\ & CWP - 1.62T^2 - 1.62pH^2 - 0.14CWP^2 \end{aligned} \quad (2)$$

Which represents the hydrogen yield (Y_{H_2}) as a function of the evaluated variables in the experimental region. The value of the regression coefficient ($R^2 = 0.91$) revealed that the regression model was an accurate representation of the experimental data, which can explain 91.0% of the variability of the dependent variable. This model was used to construct the response surface and

Table 4

ANOVA of the hydrogen yield obtained under different experimental conditions determined by the experimental design.

| Source | Sum of squares | Degrees freedom | Mean square | F-value | p-value |
|------------------|--------------------------|-----------------|-------------------------|---------|---------|
| Model | 51.04 | 9 | 5.67 | 6.98 | 0.0140 |
| T | 3.27 | 1 | 3.27 | 4.03 | 0.0915 |
| pH | 1.96 | 1 | 1.96 | 2.41 | 0.1713 |
| CWP | 0.16 | 1 | 0.16 | 0.20 | 0.6683 |
| T*pH | 0.44 | 1 | 0.44 | 0.54 | 0.4884 |
| T*CWP | 2.97 | 1 | 2.97 | 3.66 | 0.1043 |
| pH*CWP | 0.025 | 1 | 0.025 | 0.031 | 0.8668 |
| T ² | 24.20 | 1 | 24.20 | 29.80 | 0.0016 |
| pH ² | 24.20 | 1 | 24.20 | 29.80 | 0.0016 |
| CWP ² | 0.19 | 1 | 0.19 | 0.24 | 0.6417 |
| Residual | 4.87 | 6 | 0.81 | | |
| Pure error | 1.084 × 10 ⁻⁴ | 1 | 1.08 × 10 ⁻⁴ | | |
| Cor total | 55.92 | 15 | | | |

Table 5

ANOVA of the hydrogen production rate obtained under different experimental conditions determined by the experimental design.

| Source | Sum of squares | Degrees freedom | Mean square | F-value | p-value |
|------------------|-------------------------|-----------------|-------------------------|-------------------------|---------|
| Model | 50.27 | 9 | 5.59 | 7.69 | 0.0110 |
| T | 4.43 | 1 | 4.43 | 6.10 | 0.0484 |
| pH | 1.62 | 1 | 1.62 | 2.24 | 0.1855 |
| CWP | 3.83 × 10 ⁻⁴ | 1 | 3.83 × 10 ⁻⁴ | 5.27 × 10 ⁻⁴ | 0.9824 |
| T*pH | 1.40 | 1 | 1.40 | 1.93 | 0.2140 |
| T*CWP | 0.39 | 1 | 0.39 | 0.54 | 0.4888 |
| pH*CWP | 0.094 | 1 | 0.094 | 0.13 | 0.7317 |
| T ² | 24.68 | 1 | 24.68 | 33.99 | 0.0011 |
| pH ² | 24.68 | 1 | 24.68 | 33.99 | 0.0011 |
| CWP ² | 0.31 | 1 | 0.31 | 0.43 | 0.5375 |
| Residual | 4.36 | 6 | 0.73 | | |
| Pure error | 5.86 × 10 ⁻⁴ | 1 | 5.86 × 10 ⁻⁴ | | |
| Cor total | 54.63 | 15 | | | |

contour plots for hydrogen yield (Fig. 1). Fig. 1 A–B, shows the interaction of temperature and pH on hydrogen yield when the CWP concentration is fixed at 30 g dm⁻³. It is possible to observe that the highest hydrogen yield is achieved at a small range of temperature and pH. When temperature and pH are raised from 15 to 30 °C and 4.8 to 7, respectively, an increase in hydrogen yield is observed. However, a further increase to 35 °C and pH 8 leads to a marked drop on hydrogen yield. In Fig. 1C–F is easy to observe that increasing CWP concentration does not increase the hydrogen yield. Fig. 1C–D shows that the highest hydrogen yields are achieved at CWP concentrations in a range of 15 to 35 g dm⁻³ as long as temperature is maintained in a range of 22.5–30 °C. The same effect is observed in Fig. 1E–F, where initial pH must be maintained at slightly acidic to neutral conditions of 6.5–7.5. This effect can be attributed to a possible substrate inhibition at CWP concentrations above 15 g dm⁻³. High substrate concentrations trigger the accumulation of organic acids that are inhibitory to hydrogen-producing bacteria. Although in this study, the analysis of soluble metabolites produced at each experimental condition showed that the organic acids are synthesized at a low extent compared to ethanol and 2,3-butanediol, being the alcohols, the most abundant liquid metabolites produced (Table 3). Another possible reason, could be the high osmolality caused by the highest CWP concentrations, resulting in growth inhibition and incomplete substrate conversion (Ciranna et al., 2014). The pH is considered a key variable in dark fermentation processes, since it can directly affect the hydrogenase activity and metabolic pathways. The optimum pH range observed in this study is in agreement with the optimum range for hydrogen production using CW as reported by several authors. For instance, De Gioannis et al. (2014) evaluated different pH values in the

range of 5.5–8.5 using activated sludge and concluded that the optimum pH range for hydrogen production was between 6.5–7.5. Ferchichi et al. (2005) evaluated the initial pH in a range of 5–10 and found that hydrogen yield peaked at an initial pH 6. At the same time, operating temperature also has a strong influence on fermentative hydrogen production. Wang and Wan (2009) states that in an appropriate range, increasing culture temperature increases the ability of hydrogen-producing bacteria to evolve hydrogen during the fermentative process. It can be explained by the enhancement of the microbial metabolism, but an excessive temperature level affects the cell membrane integrity (Infantes et al., 2011; Raso and Barbosa-Cánovas, 2003) which inactivates the microorganism and in turn hydrogen production. Several authors have reported different hydrogen yields which can be compared with the highest yield of 1.23 ± 0.01 mol H₂ mol⁻¹ lactose achieved in this work. For instance, Rai et al. (2012) evaluated the hydrogen production at 30 °C by *E. aerogenes* MTCC 2822 using diluted raw CW at several lactose concentrations in a range of 5–40 g dm⁻³ at initial pH 6.8, achieving hydrogen yields in a range of 0.77–2.04 mol mol⁻¹ lactose. Vasmará and Marchetti (2017) reported a hydrogen yield of 1.81 mol H₂ mol⁻¹ lactose at 35 °C, initial pH 8.0 and 51 g dm⁻³ lactose using scotta permate. De Gioannis et al. (2014) evaluated different pH set-up values in a range of 5.5–8.8 achieving different hydrogen yield values from 0.04–2.6 mol H₂ mol⁻¹ lactose using anaerobic activated sludge. While Blanco et al. (2019) reported a maximum hydrogen yield of 1.4 mol mol⁻¹ lactose at 25 °C with synthetic CW at an initial chemical oxygen demand (COD) of 24 g dm⁻³. The yield achieved by *E. asburiae* is within the range reported by these authors. The theoretical hydrogen yield using lactose is 8 mol H₂ mol⁻¹ lactose, however lower yields are achieved in practice. This stoichiometric yield is only attainable under near-equilibrium conditions, which implies very slow hydrogen rates and/or at very low hydrogen partial pressure (HPP) (Nath and Das, 2004). As HPP increases, hydrogen synthesis decreases and metabolic pathways shifts toward production of more reduced substrates, such as lactate and alcohols (Hallenbeck and Benemann, 2002; Nath and Das, 2004). In this study, high substrate concentrations used may have provided high HPP which contributed to the low hydrogen yields achieved by the experiments with high level of CWP concentration (exp. 12, 13, 14, 15 and 16). At a metabolic level, low hydrogen yields indicate the presence of hydrogen competing pathways. In bacteria belonging to *Enterobacter* genus, hydrogen production is carried out through two ways, one is dependent of the cleavage of pyruvate into formate and Acetyl-CoA and the other one depends on the oxidation of NADH (Lu et al., 2009). Therefore, the conversion of phosphoenol-pyruvate and pyruvate into reduced acids such as succinate and lactate, as well as alcohols such as ethanol and 2,3-butanediol, reduces significantly the hydrogen yield. In Table 3, the different soluble metabolites produced by *E. asburiae* at each experimental condition are shown. As noted, 2,3-butanediol and ethanol are the most abundant metabolites. Therefore, the hydrogen yield by *E. asburiae* was affected by the synthesis of these compounds. This could be further improved applying metabolic engineering over these competing pathways.

3.2. Hydrogen production rate under different operating conditions

Along with hydrogen yield, the rate of hydrogen production is another relevant variable to be evaluated in fermentative hydrogen production processes. Together, these two variables indicate the feasibility of the process. Thus, hydrogen production rate was also chosen as a response variable. Table 2 shows the different experimental conditions evaluated with the corresponding hydrogen production rate results. In the same way as with the

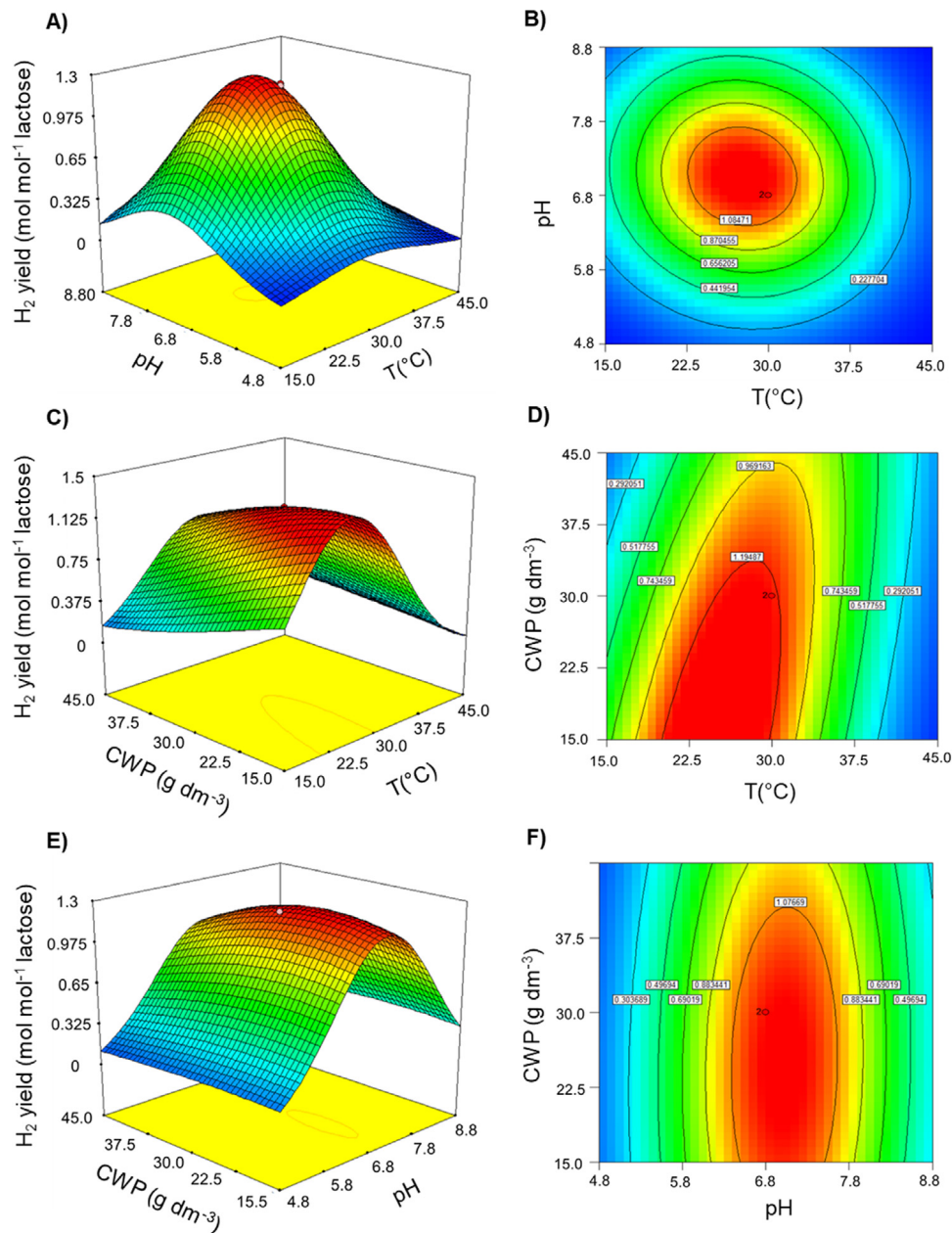


Fig. 1. Different response surface and contour plots of the effects of temperature, initial pH and CWP concentration on hydrogen yield by *E. asburiae*. (A–B) CWP concentration was fixed at 30 g dm^{-3} , (C–D) initial pH was maintained at 6.8 and in (E–F) temperature was kept at $30 \text{ }^\circ\text{C}$.

hydrogen yield model, a natural Log transformation was applied to ensure that the model meets the assumptions required for ANOVA. The factors that significantly ($p < 0.05$) affected the hydrogen production rate were the linear and quadratic effect of temperature, and the quadratic effect of pH (Table 5). The highest hydrogen production rate ($10.41 \pm 0.25 \text{ cm}^3 \text{ dm}^{-3} \text{ h}^{-1}$) was achieved at the central points of the experimental design (Exp. 8 and 9) at $30 \text{ }^\circ\text{C}$, initial pH 6.8 and 30 g dm^{-3} CWP. While a decrease in the rates was observed in experiments 1 and 16 (5.65 and $6.96 \text{ cm}^3 \text{ dm}^{-3} \text{ h}^{-1}$, respectively) at the axial points of CWP concentration (4.8 and 55.2 g dm^{-3}), $30 \text{ }^\circ\text{C}$ and initial pH 6.8. Lower rates in a range of 0.10 – $2.91 \text{ cm}^3 \text{ dm}^{-3} \text{ h}^{-1}$ were obtained in experiments 12, 14 and 15 using 45 g dm^{-3} CWP and in experiments 2 and 4 at $15 \text{ }^\circ\text{C}$ and 15 g dm^{-3} CWP. Whereas the absence of hydrogen production was observed in the experiments 7, 10, 6 and 11 with the axial points of temperature and pH, as well as for experiments 3, 5 and 13 at a high temperature of $45 \text{ }^\circ\text{C}$.

The final second-order-polynomial in terms of the coded factors after the natural Log transformation is expressed as follows:

$$\begin{aligned} \ln(HPR + 0.11) = & 2.36 - 0.57T + 0.34pH - 0.0053CWP \\ & - 0.42T * pH + 0.22T * \\ & CWP + 0.11pH * CWP - 1.63T^2 - 1.63pH^2 - 0.18CWP^2 \end{aligned} \quad (3)$$

Eq. (3) represents the hydrogen production rate (HPR) as a function of the evaluated variables in the experimental region. The value of regression coefficient ($R^2 = 0.92$) revealed that the model was an accurate representation of the experimental data, which can explain 92% of the variability of the dependent variable. This model was used to construct the response surface and contour plots for hydrogen production rate (Fig. 2). As noted in Fig. 2, the effect of temperature, initial pH and CWP concentration followed the same trend as in the hydrogen yield model. Fig. 2 A–B shows that the highest production rate is achieved when

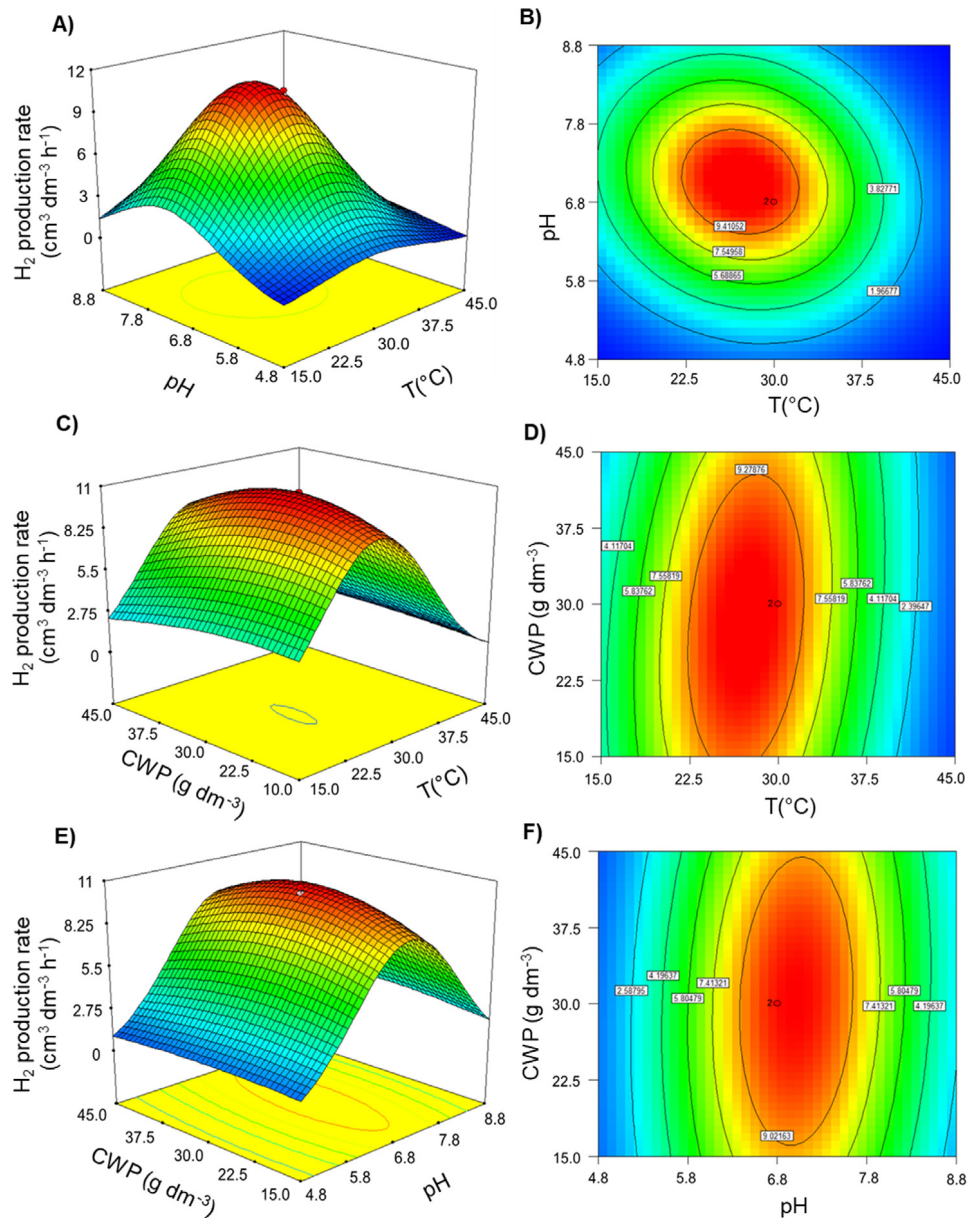


Fig. 2. Different response surface and contour plots of the effects of temperature, initial pH and CWP concentration on hydrogen production rate by *E. asburiae*. (A–B) CWP concentration was fixed at 30 g dm^{-3} , (C–D) initial pH was maintained at 6.8 and in (E–F) temperature was kept at $30 \text{ }^\circ\text{C}$.

temperature and pH are increased to $30 \text{ }^\circ\text{C}$ and 7, respectively. Temperature has a direct effect on the reaction rate; an oft-cited general rule states that a $10 \text{ }^\circ\text{C}$ rise in temperature will double the rate of reactions (Slowinski et al., 2004). Therefore, the increase from $15 \text{ }^\circ\text{C}$ to $30 \text{ }^\circ\text{C}$ resulted beneficial for the hydrogen production rate. However, when temperature is increased above $30 \text{ }^\circ\text{C}$ a decline in the curve was observed. At higher temperatures than the optimum value, some essential enzymes and proteins associated with cell growth or hydrogen production (hydrogenases) may be inactivated (or denatured) (Lee et al., 2006). As mentioned before, pH is another factor that influence the activity of the hydrogenases and the metabolic functions of bacteria. Low pH values give poor hydrogen production rates since these values have an initial inhibitory effect on bacteria causing longer lag phases (Skonieczny and Yargeau, 2009). Fig. 3 E–F shows that when initial pH increases to a range of 6.5–7, a maximum hydrogen production rate is achieved, moreover, it is evident that the increase of substrate concentration from 15 to 45 g dm^{-3} CWP shows no difference on hydrogen production rate under the

optimum initial pH range. However, CWP concentrations below 15 g dm^{-3} or exceeding 45 g dm^{-3} lead to a fall in the production rate. According to Lu et al. (2018), substrate concentration below the optimum value always leads to low hydrogen production rate, hydrogen content and biomass concentration, on the other hand, when substrate concentration is higher than its optimum value, hydrogen-producing microorganisms could overproduce volatile fatty acids and alcohols leading to decreased hydrogen production rates. In literature, different hydrogen production rates from CW are reported using different fermentation configurations, conditions and inocula. The maximum hydrogen production rate achieved in this work is within the range of the reported values in the literature. For instance, Kargi et al. (2012) evaluated the hydrogen production from CWP by anaerobic sludge in batch serological bottles, where the highest hydrogen production of $3.46 \text{ cm}^3 \text{ dm}^{-3} \text{ h}^{-1}$ was obtained at the thermophilic conditions of $55 \text{ }^\circ\text{C}$ and pH 7, whereas in this study, the highest production rate of $10.59 \text{ cm}^3 \text{ dm}^{-3} \text{ h}^{-1}$ was achieved. Ghimire et al. (2017) evaluated the co-fermentation of CW with buffalo manure as

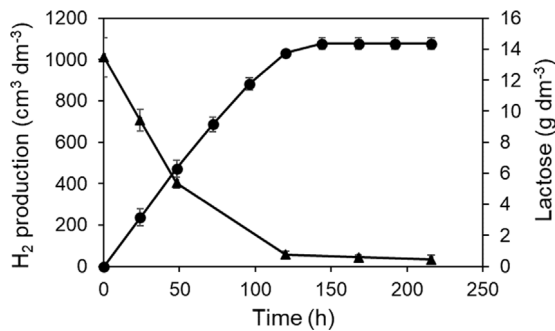


Fig. 3. Hydrogen production (circles) and lactose consumption (triangles) kinetics by *E. asburiae* under the optimum conditions of 25.6 °C, initial pH 7.2 and 23.0 g dm⁻³ CWP. The error bars indicate standard deviations.

buffering agent in a semi-continuous reactor at 55 °C and pH 4.8–5.0 reporting a production rate of 8.97 cm³ dm⁻³ h⁻¹. Likewise, Lopes et al. (2017) reported the co-fermentation of CW and crude glycerol in an expanded granular sludge bed at 30 °C and pH 8.7–9.0 reaching a higher production rate of 42.5 cm³ dm⁻³ h⁻¹. Perna et al. (2013) observed a similar rate of 41.66 cm³ dm⁻³ h⁻¹ using an up-flow anaerobic packed bed reactor at 30 °C and pH 5.6 with a mixed culture.

3.3. Optimization and validation of the optimum conditions

The simultaneous optimization of the two response variables evaluated in this study was carried out using the Design Expert v7.0 software. The maximum hydrogen yield and hydrogen production rate predicted by the model were 1.37 mol mol⁻¹ lactose and 10.79 cm³ dm⁻³ h⁻¹, respectively at the optimum conditions of 25.6 °C, initial pH 7.2 and 23.0 g dm⁻³ CWP. The accuracy of the model was validated by performing an additional set of batch fermentations by triplicate under the optimum conditions (Fig. 3). The experimental results obtained for hydrogen yield and hydrogen production rate were 1.19 ± 0.01 mol H₂ mol⁻¹ lactose and 9.34 ± 0.22 cm³ dm⁻³ h⁻¹, respectively, which are close to the values predicted by the model, indicating that RSM was a useful tool to optimize the response variables.

3.4. Production of soluble metabolites

The main soluble metabolites produced in the different experimental conditions were succinic acid, lactic acid, formic acid, acetic acid, 2,3-butanediol and ethanol (Table 3). The distribution of these metabolic products was certainly influenced by the combined effect of the operating conditions. The RSM is an effective tool to evaluate simultaneously the effect of multiple factors on dark fermentation (Wang and Wan, 2008), however, the analysis of the data set can be improved by the application of chemometric tools such as HCA and PCA. These techniques allow an easy statistical and visual interpretation of complex data relationships frequently encountered in multivariate analysis, since they describe the similarities and differences between the set of variables (Upadhyay et al., 2017). Therefore, the production of the soluble metabolites was analyzed using these chemometric tools.

3.4.1. Chemometric analysis of the soluble metabolites produced during hydrogen production

3.4.1.1. Principal component analysis (PCA). PCA model with four significant principal components (PCs) described 96.67% of the total data variance. Score plots and loading plots obtained as a result of the analysis are presented in Fig. 4. PC1, which described 47.66% of the total variance was constructed mainly due to the

differences between the object 8 (30 °C, pH 6.8 and 30 g dm⁻³ CWP) and all the remaining objects (Table 3). Moreover, along the PC1 the objects can be divided into three clusters and one non-grouped object 5 (45 °C, pH 8.8 and 15 g dm⁻³ CWP). The first cluster was composed of objects 2, 4, 9 and 11. The second cluster was composed of the objects 1, 3, 6, 10 and 12, while the third cluster was composed of objects 7, 8 and 13. Based on the interpretation of Fig. 4, it may be concluded that object 8 was characterized by relatively high concentration of lactic acid and 2,3-butanediol and the lowest concentration of formic acid. The objects included in the first cluster were characterized by relatively high concentrations of formic acid and 2,3-butanediol. The PC2, describing 26.92% of the total data variance was constructed due to the differences between the object 4, which was unique due to high concentration of ethanol and object 6 characterized by the lowest concentration of ethanol and high concentration of lactic acid. Moreover, along the PC2 it may be observed that objects 1, 5, 6, 10 and 12 were unique because of relatively high concentration of lactic acid and lower concentrations of all the remaining metabolites. The PC4, describing 6.91% of the total data variance was constructed because of the differences between object 3 and all the remaining objects. The object 3 differed from all the remaining objects in terms of the highest concentration of formic acid and low concentrations of 2,3-butanediol and ethanol. Although the metabolites were effectively segregated by PCA, their possible similarities were not greatly illustrated. Therefore, for a more in-depth analysis of the effect of temperature, initial pH and CWP concentration on the distribution of the metabolites, the HCA complemented with a visual display of the data was applied. HCA is a powerful chemometric tool used to discover the inherent grouping and distribution in the data set (Upadhyay et al., 2017).

3.4.1.2. Hierarchical cluster analysis (HCA). The dendrograms constructed with the application of the Ward's linkage method are presented in Fig. 5. The Euclidean distance was employed as the similarity measure.

The dendrogram presented in Fig. 5A revealed three clusters: A, B and C of different experimental conditions.

- Cluster A composed of the objects 1, 3, 5, 6, 7, 10, 11, 13 and 15.
- Cluster B composed of the objects 2, 4, 12 and 14.
- Cluster C composed of the objects 8, 9 and 16.

Within the main clusters the following sub-clustering structures may be distinguished: two sub-clusters within cluster A (A1 and A2) and one sub-cluster within cluster B (B1):

- Sub-cluster A1 composed of the objects 6, 7, 10 and 11.
- Sub-cluster A2 composed of the objects 1, 3, 5, 16 and 15.
- Sub-cluster B1 composed of the objects 2, 4 and 12.

The dendrograms constructed for the metabolites produced during the fermentation under various operating conditions (Fig. 5B) revealed two main classes:

- Class A containing parameters 1, 2, 4 and 5 (corresponding to lactic acid, succinic acid, acetic acid and 2,3-butanediol, respectively).
- Class B containing parameters 3, and 6 (corresponding to formic acid and ethanol, respectively).

The results obtained from the analysis of the dendrograms presented in Fig. 5A–B show the data structure but did not allow interpreting the observed patterns in terms of parameters. To solve this problem the color map of the studied data was employed (Fig. 5C). A simultaneous analysis of the dendrograms of studied

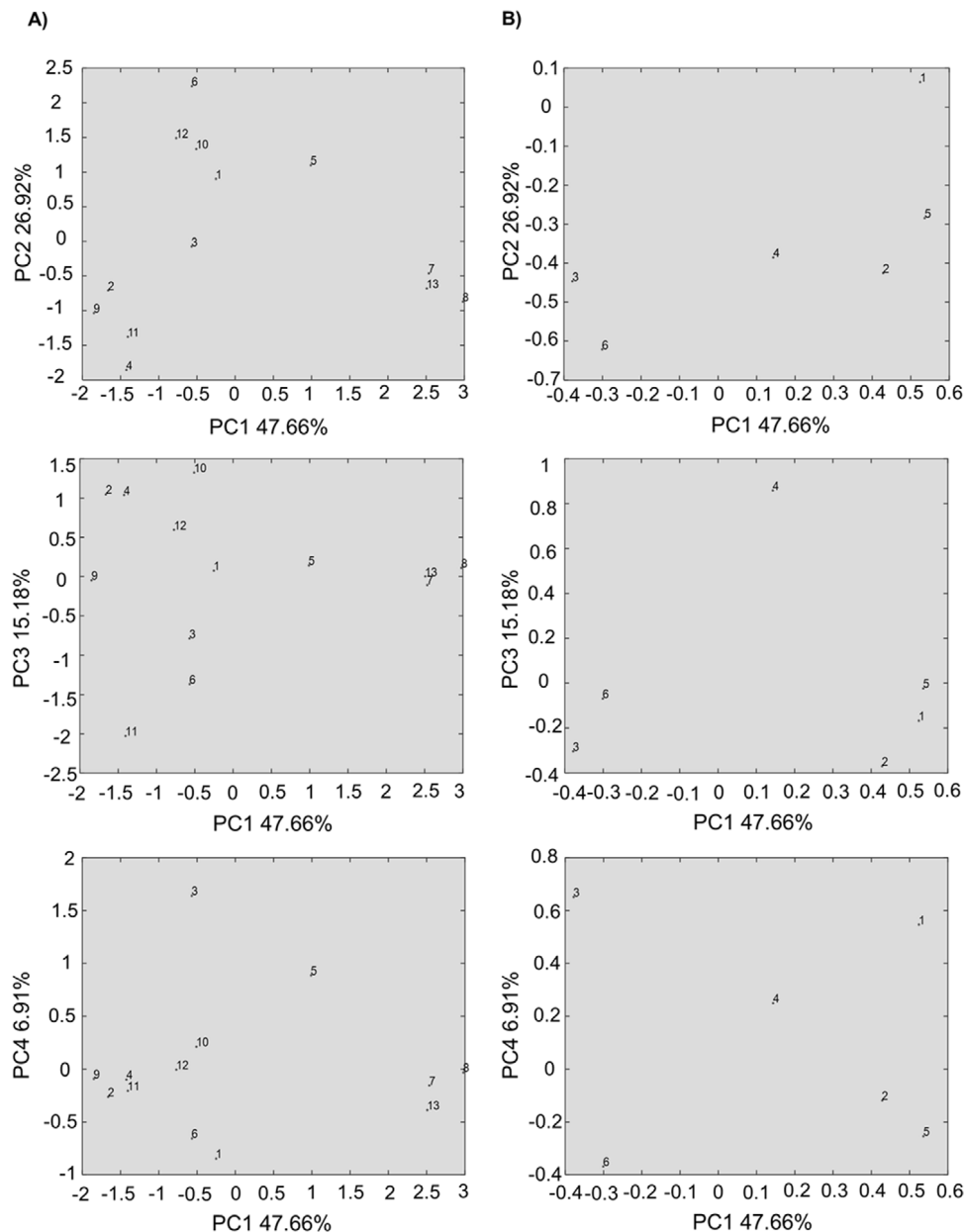


Fig. 4. (A) Score plots and (B) loading plots of PCA for centered and standardized data set X (16 x 6).

test of the experimental conditions in the parameters space with the color map of data allowed a more in-depth exploration of the relationships among the studied experiments. Particularly, the objects grouped in cluster A differed from the remaining ones mainly in terms of low concentration of 2,3-butanediol and ethanol (parameters 5 and 6, respectively). The objects in sub-cluster A1 correspond to the axial points of temperature and pH (4.8 and 55.2 °C and pH 3.4 and 10.1, respectively), which are additional experiments at a α distance from the central point. These experiments allowed to estimate the curvature of the response surface; therefore, they constitute the lowest and the highest conditions of temperature and pH on the experimental design. While the four objects in sub-cluster A2 correspond to the experiments at temperature of 45 °C. The absence of alcohol and the low production of the other metabolites can be attributed to the detrimental effect of the extreme conditions of these experiments. The difference between sub-clusters A1 and A2 is the higher concentration of acetic acid (parameter 4) in the latter. Also, within sub-cluster A2, the uniqueness of objects

3 and 5 was observed due to the high concentrations of lactic acid and formic acid. Subsequently, Cluster B is composed by four objects, which were carried out at a low temperature of 15 °C. The uniqueness of this cluster was related to high concentration of formic acid and acetic acid, as well as ethanol (parameters 3, 4 and 6), which indicates that these conditions were the most suitable for the formate hydrogen lyase complex activity, which is responsible for the breakdown of pyruvate into formate and acetyl-CoA (Ji et al., 2011). On the other hand, the accumulation of formic acid suggests that the hydrogen evolving hydrogenases were partially inhibited during fermentation. Sub-cluster B1 was characterized by the highest concentrations of ethanol (parameter 6). In addition, within the cluster B, the uniqueness of object 4 was also observed caused by the highest concentration of acetic acid (parameter 4) among all objects. Finally, cluster C, which is composed by three objects, is characterized by the highest concentrations of succinic acid and 2,3-butanediol (parameters 2 and 5) among all the studied objects. Also, it is characterized by a high concentration of lactic acid and low concentrations of formic

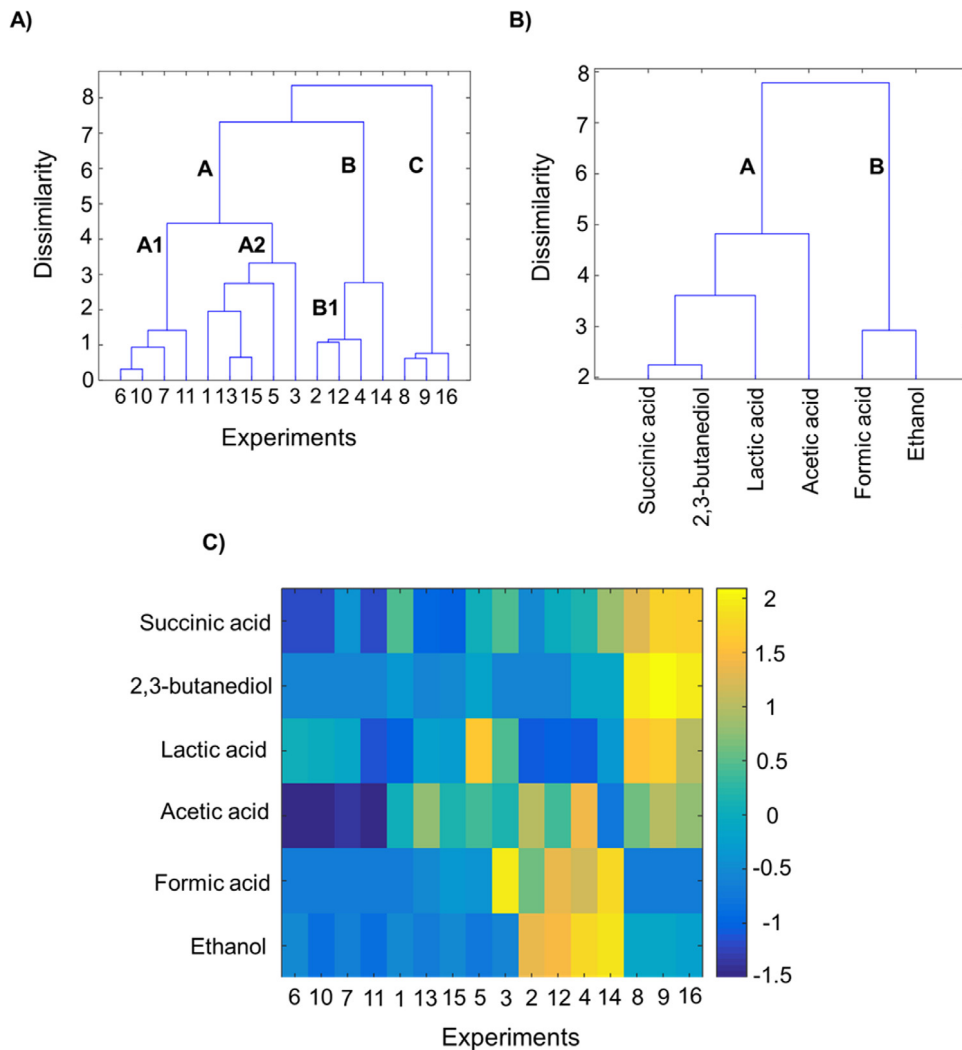


Fig. 5. Dendrograms of (A) studied objects (experiments of hydrogen production under various conditions), (B) parameters (metabolites produced during CWP dark fermentation) in the objects space based on the Ward's linkage method and using the Euclidean distance as the similarity measure with (C) the color map of the studied data sorted according to the Ward's linkage method.

acid and ethanol. This information suggests that the operating conditions of the objects in cluster C, stimulated the carbon flux through the first branches of the mixed acid pathway, where the involved reactions are used for the disposal of the reducing power generated by the catabolism of the lactose present in the CWP. Also, it indicates that most of the hydrogen produced on these conditions, was through the NADH pathway. As well, the pH values of 6.8 in this cluster could have favored the synthesis of 2,3-butanediol, since it is known that the α -acetolactate synthase enzyme, which is one of the three key enzymes involved on 2,3-butanediol synthesis, has an optimum activity under slightly acidic conditions of 6 (Celińska and Grajek, 2009).

4. Conclusions

RSM along with the PCA and HCA, allowed to identify in a more depth way the influence of key operating parameters such as temperature, initial pH and CWP concentration on hydrogen yield and soluble metabolites produced by *E. asburiae*. The RSM allowed estimating the optimum conditions for hydrogen yield and production rate (25.6 °C, initial pH 7.2 and 23.0 g dm⁻³ CWP), as well as to identify the individual and conjugated effect of the factors on these response variables. According to the ANOVA of the models, only the quadratic terms of temperature and pH

influenced hydrogen yield. While hydrogen production rate was affected by the linear and quadratic effect of temperature and the quadratic effect of pH. On the other hand, PCA and HCA allowed reducing the dimensionality of the data of the metabolites produced, thus allowing a better visualization and interpretation of the distribution of the organic acids and alcohols on response of each condition evaluated. The fact that CWP fermentation by *E. asburiae* produced mainly hydrogen and alcohols, it could be exploited in later studies as a biorefinery concept.

CRedit authorship contribution statement

Cecilia L. Alvarez-Guzmán: Investigation, Resources, Writing - original draft. **Sergio Cisneros-de la Cueva:** Investigation, Resources, Writing - original draft. **Victor E. Balderas-Hernández:** Data curation, Supervision. **Adam Smoliński:** Formal analysis, Methodology. **Antonio De León-Rodríguez:** Conceptualization, Writing - review & editing, Project administration, Funding acquisition.

Declaration of competing interest

The authors declare that they have no known competing financial interests or personal relationships that could have appeared to influence the work reported in this paper.

Acknowledgments

The authors thank to CONACyT, Mexico Ciencias Básicas 281700 for the financial support. C.L. Alvarez-Guzmán thanks to CONACyT, Mexico for her scholarship 330870.

References

- Azbar, N., Dökgoz, F.T.Ç., Peker, Z., 2009. Optimization of basal medium for fermentative hydrogen production from cheese whey wastewater. *Int. J. Green Energy* 6, 371–380. <http://dx.doi.org/10.1080/15435070903107049>.
- Bao, M., Su, H., Tan, T., 2012. Biohydrogen production by dark fermentation of starch using mixed bacterial cultures of *Bacillus* sp and *Brevundimonas* sp. *Energy Fuels* 26, 5872–5878. <http://dx.doi.org/10.1021/ef300666m>.
- Blanco, V.M.C., Oliveira, G.H.D., Zaiat, M., 2019. Dark fermentative biohydrogen production from synthetic cheese whey in an anaerobic structured-bed reactor: Performance evaluation and kinetic modeling. *Renew. Energy* 139, 1310–1319. <http://dx.doi.org/10.1016/j.renene.2019.03.029>.
- Celińska, E., Grajek, W., 2009. Biotechnological production of 2, 3-butanediol—Current state and prospects. *Biotechnol. Adv.* 27, 715–725. <http://dx.doi.org/10.1016/j.biotechadv.2009.05.002>.
- Ciranna, A., Ferrari, R., Santala, V., Karp, M., 2014. Inhibitory effects of substrate and soluble end products on biohydrogen production of the alkalithermophile *Caloramator celer*: Kinetic, metabolic and transcription analyses. *Int. J. Hydrog. Energy* 39, 6391–6401. <http://dx.doi.org/10.1016/j.ijhydene.2014.02.047>.
- da Silva Veras, T., Mozer, T.S., da Costa Rubim Messeder dos Santos, D., da Silva César, A., 2017. Hydrogen: Trends, production and characterization of the main process worldwide. *Int. J. Hydrog. Energy* 42, 2018–2033. <http://dx.doi.org/10.1016/j.ijhydene.2016.08.219>.
- De Gianninis, G., Friargiu, M., Massi, E., Muntoni, A., Polettini, A., Pomi, R., Spiga, D., 2014. Biohydrogen production from dark fermentation of cheese whey: Influence of pH. *Int. J. Hydrog. Energy* 39, 20930–20941. <http://dx.doi.org/10.1016/j.ijhydene.2014.10.046>.
- Djaković Sekulić, T., Božin, B., Smoliński, A., 2016. Chemometric study of biological activities of 10 aromatic Lamiaceae species' essential oils. *J. Chemom.* 30, 188–196. <http://dx.doi.org/10.1002/cem.2786>.
- Ferchichi, M., Crabbe, E., Gil, G.H., Hintz, W., Almadidy, A., 2005. Influence of initial pH on hydrogen production from cheese whey. *J. Biotechnol.* 120, 402–409. <http://dx.doi.org/10.1016/j.jbiotec.2005.05.017>.
- Gentle, J.E., Kaufman, L., Rousseuw, P.J., 1991. Finding groups in data: An introduction to cluster analysis. *Biometrics* 47, 788. <http://dx.doi.org/10.2307/2532178>.
- Ghimire, A., Luongo, V., Frunzo, L., Pirozzi, F., Lens, P.N.L., Esposito, G., 2017. Continuous biohydrogen production by thermophilic dark fermentation of cheese whey: Use of buffalo manure as buffering agent. *Int. J. Hydrog. Energy* 42, 4861–4869. <http://dx.doi.org/10.1016/j.ijhydene.2016.11.185>.
- Gunst, R.F., Myers, R.H., Montgomery, D.C., 1996. Response surface methodology: Process and product optimization using designed experiments. *Technometrics* 38, 285. <http://dx.doi.org/10.2307/1270613>.
- Hallenbeck, P.C., Benemann, J.R., 2002. Biological hydrogen production; Fundamentals and limiting processes. In: *International Journal of Hydrogen Energy*. Pergamon, pp. 1185–1193. [http://dx.doi.org/10.1016/S0360-3199\(02\)00131-3](http://dx.doi.org/10.1016/S0360-3199(02)00131-3).
- Holladay, J.D., Hu, J., King, D.L., Wang, Y., 2009. An overview of hydrogen production technologies. *Catal. Today* 139, 244–260. <http://dx.doi.org/10.1016/j.cattod.2008.08.039>.
- Howaniec, N., Smoliński, A., Cempa-Balewicz, M., 2015. Experimental study on application of high temperature reactor excess heat in the process of coal and biomass co-gasification to hydrogen-rich gas. *Energy* 84, 455–461. <http://dx.doi.org/10.1016/j.energy.2015.03.011>.
- Infantes, D., González Del Campo, A., Villaseñor, J., Fernández, F.J., 2011. Influence of pH, temperature and volatile fatty acids on hydrogen production by acidogenic fermentation. *Int. J. Hydrog. Energy* 36, 15595–15601. <http://dx.doi.org/10.1016/j.ijhydene.2011.09.061>.
- Ji, X., Huang, H., Ouyang, P., 2011. Microbial 2, 3-butanediol production: a state-of-the-art review. *Biotechnol. Adv.* 29, 351–364. <http://dx.doi.org/10.1016/j.biotechadv.2011.01.007>.
- Jolliffe, I., 2002. Principal component analysis. In: *Series: Springer Series in Statistics*, vol. 29, Springer New York, NY, p. 487.
- Kargi, F., Eren, N.S., Ozmihi, S., 2012. Bio-hydrogen production from cheese whey powder (CWP) solution: Comparison of thermophilic and mesophilic dark fermentations. *Int. J. Hydrog. Energy* 37, 8338–8342. <http://dx.doi.org/10.1016/j.ijhydene.2012.02.162>.
- Kargi, F., Ozmihi, S., 2006. Utilization of cheese whey powder (CWP) for ethanol fermentations: Effects of operating parameters. *Enzyme Microb. Technol.* 38, 711–718. <http://dx.doi.org/10.1016/j.enzmictec.2005.11.006>.
- Lee, D.H., 2017. Econometric assessment of bioenergy development. *Int. J. Hydrog. Energy* 42, 27701–27717. <http://dx.doi.org/10.1016/j.ijhydene.2017.08.055>.
- Lee, K.S., Lin, P.J., Chang, J.S., 2006. Temperature effects on biohydrogen production in a granular sludge bed induced by activated carbon carriers. *Int. J. Hydrog. Energy* 31, 465–472. <http://dx.doi.org/10.1016/j.ijhydene.2005.04.024>.
- Lopes, H.J.S., Ramos, L.R., Silva, E.L., 2017. Co-fermentation of cheese whey and crude glycerol in EGSB reactor as a strategy to enhance continuous hydrogen and propionic acid production. *Appl. Biochem. Biotechnol.* 183, 712–728. <http://dx.doi.org/10.1007/s12010-017-2459-7>.
- Lu, C., Zhang, Z., Zhou, X., Hu, J., Ge, X., Xia, C., Zhao, J., Wang, Y., Jing, Y., Li, Y., Zhang, Q., 2018. Effect of substrate concentration on hydrogen production by photo-fermentation in the pilot-scale baffled bioreactor. *Bioresour. Technol.* 247, 1173–1176. <http://dx.doi.org/10.1016/j.biortech.2017.07.122>.
- Lu, Y., Zhao, H., Zhang, C., Lai, Q., Wu, X., Xing, X.H., 2009. Expression of nad⁺-dependent formate dehydrogenase in *Enterobacter aerogenes* and its involvement in anaerobic metabolism and H₂ production. *Biotechnol. Lett.* 31, 1525–1530. <http://dx.doi.org/10.1007/s10529-009-0036-z>.
- Manuel Rosales-Colunga, L., Donaxí Alvarado-Cuevas, Z., Razo-Flores, Elías, De León Rodríguez, Antonio, Rosales-Colunga, L.M., Alvarado-Cuevas, Z.D., De León Rodríguez, A., León Rodríguez, Antonio, Razo-Flores, E., 2013. Maximizing hydrogen production and substrate consumption by *Escherichia coli* WDH1 in cheese whey fermentation. *Appl. Biochem. Biotechnol.* 171, 704–715. <http://dx.doi.org/10.1007/s12010-013-0394-9>.
- Milligan, G.W., Romesburg, H.C., 1985. Cluster analysis for researchers. *J. Mark. Res.* 22, 224. <http://dx.doi.org/10.2307/3151374>.
- Mohan, S.V., Chandrasekhar, K., Chiranjeevi, P., Babu, P.S., 2013. Biohydrogen production from wastewater. In: *Biohydrogen*. pp. 223–257. <http://dx.doi.org/10.1016/B978-0-444-59555-3.00010-6>.
- Nath, K., Das, D., 2004. Improvement of fermentative hydrogen production: Various approaches. *Appl. Microbiol. Biotechnol.* <http://dx.doi.org/10.1007/s00253-004-1644-0>.
- Perna, V., Castelló, E., Wenzel, J., Zampol, C., Fontes Lima, D.M., Borzacconi, L., Varesche, M.B., Zaiat, M., Etchebehere, C., 2013. Hydrogen production in an upflow anaerobic packed bed reactor used to treat cheese whey. *Int. J. Hydrog. Energy* 38, 54–62. <http://dx.doi.org/10.1016/j.ijhydene.2012.10.022>.
- Prazeres, A.R., Carvalho, F., Rivas, J., 2012. Cheese whey management: A review. *J. Environ. Manag.* 110, 48–68. <http://dx.doi.org/10.1016/j.jenvman.2012.05.018>.
- Rai, P.K., Singh, S.P., Asthana, R.K., 2012. Biohydrogen production from cheese whey wastewater in a two-step anaerobic process. *Appl. Biochem. Biotechnol.* 167, 1540–1549. <http://dx.doi.org/10.1007/s12010-011-9488-4>.
- Raso, J., Barbosa-Cánovas, G.V., 2003. Nonthermal preservation of foods using combined processing techniques. *Crit. Rev. Food Sci. Nutr.* 43, 265–285. <http://dx.doi.org/10.1080/10408690390826527>.
- Rosales-Colunga, L.M., Razo-Flores, E., Ordoñez, L.G., Alariste-Mondragón, F., De León-Rodríguez, A., 2010. Hydrogen production by *Escherichia coli* ΔhycA ΔlacI using cheese whey as substrate. *Int. J. Hydrog. Energy* 35, 491–499. <http://dx.doi.org/10.1016/j.ijhydene.2009.10.097>.
- Ryan, M.P., Walsh, G., 2016. The biotechnological potential of whey. *Rev. Environ. Sci. Biotechnol.* 15, 479–498. <http://dx.doi.org/10.1007/s11157-016-9402-1>.
- Skonieczny, M.T., Yargeau, V., 2009. Biohydrogen production from wastewater by *Clostridium beijerinckii*: Effect of pH and substrate concentration. *Int. J. Hydrog. Energy* 34, 3288–3294. <http://dx.doi.org/10.1016/j.ijhydene.2009.01.044>.
- Slowinski, E., Wolsey, W., Masterton, W., 2004. *Chemical Principles in the Laboratory*.
- Smoliński, A., 2008. Gas chromatography as a tool for determining coal chars reactivity in the process of steam gasification. *Acta Chromatogr.* 20, 349–365. <http://dx.doi.org/10.1556/ACHrom.20.2008.3.4>.
- Smoliński, A., 2011. Coal char reactivity as a fuel selection criterion for coal-based hydrogen-rich gas production in the process of steam gasification. In: *Energy Conversion and Management*. pp. 37–45. <http://dx.doi.org/10.1016/j.enconman.2010.06.027>.
- Smoliński, A., 2014. Analysis of the impact of physicochemical parameters characterizing coal mine waste on the initialization of self-ignition process with application of cluster analysis. *J. Sustain. Min.* 13, 36–40. <http://dx.doi.org/10.7424/jsm140306>.
- Upadhyay, R., Sehwal, S., Niwas Mishra, H., 2017. Chemometric approach to develop frying stable sunflower oil blends stabilized with oleoresin rosemary and ascorbyl palmitate. *Food Chem.* 218, 496–504. <http://dx.doi.org/10.1016/j.foodchem.2016.09.105>.
- Vasmara, C., Marchetti, R., 2017. Initial pH influences in-batch hydrogen production from scotta permeate. *Int. J. Hydrog. Energy* 42, 14400–14408. <http://dx.doi.org/10.1016/j.ijhydene.2017.04.067>.
- Wang, J., Wan, W., 2008. Optimization of fermentative hydrogen production process by response surface methodology. *Int. J. Hydrog. Energy* 33, 6976–6984. <http://dx.doi.org/10.1016/j.ijhydene.2008.08.051>.

- Wang, J., Wan, W., 2009. Factors influencing fermentative hydrogen production: A review. *Int. J. Hydrog. Energy* 34, 799–811. <http://dx.doi.org/10.1016/j.ijhydene.2008.11.015>.
- Wold, S., Esbensen, K., Geladi, P., 1987. Principal component analysis. *Chemom. Intell. Lab. Syst.* 2, 37–52. [http://dx.doi.org/10.1016/0169-7439\(87\)80084-9](http://dx.doi.org/10.1016/0169-7439(87)80084-9).
- Zhou, X., Hua, X., Huang, L., Xu, Y., 2019. Bio-utilization of cheese manufacturing wastes (cheese whey powder) for bioethanol and specific product (galactonic acid) production via a two-step bioprocess. *Bioresour. Technol.* 272, 70–76. <http://dx.doi.org/10.1016/j.biortech.2018.10.001>.